Biochemistry and Biophysics Reports 42 (2025) 101981

Contents lists available at ScienceDirect

Biochemistry and Biophysics Reports

journal homepage: www.elsevier.com/locate/bbrep

Effects of the number of ethylene glycol units on the efficacy of novel complex I inhibitor 9bw

Kazuaki Sekimoto [a], Hanaka Kinjo [b], Mizuki Murakami [b], Akiko Ohashi [a,c], Rei Fukui [d], Eri Nagasaki-Maeoka [e], Yoshinori Inagaki [f], Tadateru Takayama [f], Kazuhiro Ikeda [g], Ken-ichi Takayama [h], Satoshi Inoue [g,h], Motonori Tsuji [i], Joe Otsuki [b,*], Kyoko Fujiwara [a,c,**]

[a] Department of Anatomy, Nihon University School of Dentistry, Chiyoda-ku, Tokyo, 101-8310, Japan
[b] Department of Materials and Applied Chemistry, College of Science and Technology, Nihon University, Chiyoda-ku, Tokyo, 101-8308, Japan
[c] Division of Functional Morphology, Dental Research Center, Nihon University School of Dentistry, Chiyoda-ku, Tokyo, 101-8310, Japan
[d] Department of Pathology, Nihon University School of Dentistry, Chiyoda-ku, 101-8310, Japan
[e] Department of Pediatric Surgery, Jichi Medical University, Saitama Medical Center, Saitama, 330-8503, Japan
[f] Division of General Medicine, Department of Medicine, Nihon University School of Medicine, Itabashi-ku, Tokyo, 173-0032, Japan
[g] Division of Systems Medicine & Gene Therapy, Saitama Medical University, Hidaka, Saitama, 350-1241, Japan
[h] Department of Systems Aging Science and Medicine, Tokyo Metropolitan Institute for Geriatrics and Gerontology, 35-2 Sakae-cho, Itabashi-ku, Tokyo, 173-0015, Japan
[i] Institute of Molecular Function, 2-105-14, Takasu, Misato-shi, Saitama, 341-0037, Japan

ARTICLE INFO

Keywords:
Respiratory complex I
9bw
4′-iodobiphenyl
Ethylene glycol
Oral squamous cell carcinoma

ABSTRACT

4′-Iodobiphenyl nonaethylene glycol ether (9bw) is a novel small molecule, composed of a biphenyl unit and 9 ethylene glycol (EG) units. Recently, we found that 9bw induces apoptosis in cancer cells by inhibiting mitochondrial respiratory complex I (CI) and accordingly reducing cellular ATP level. In addition, 9bw shows little effect on normal cells, suggesting that 9bw is a potential antitumor agent with few adverse effects. However, the exact molecular mechanisms by which 9bw acts on CI are still elusive. To clarify the molecular structure critical for 9bw's function, we tested the function of 9bw analogues on human oral squamous cell carcinoma lines HSC4 and Ca9-22. The analogues were 4-hydroxy-4′-iodobiphenyl (HIOP), I-BP-EG3, I-BP-EG6, and I-BP-EG12 containing 0, 3, 6, and 12 EG units, respectively. Our results demonstrated that I-BP-EG6 and I-BP-EG12 inhibited CI to a similar extent as 9bw, whereas I-BP3 and HIOP showed no effect on CI activity. These observations indicate that the number of EG units is crucial for the activity of 9bw and its analogues. As high-performance liquid chromatography (HPLC) analysis demonstrated that both HIOP and I-BP-EG3 could be incorporated into mitochondria abundantly, the number of EG units probably affects CI inhibitory function of 9bw and its analogues rather than their efficacy to enter cell and mitochondria.

1. Introduction

Cancer cells exhibit metabolic alterations to ensure their upregulated biosynthesis and cell growth. One of the most important changes is the Warburg effect, where cells tend to favor increased glycolysis and/or glucose uptake under normal oxygen conditions [1,2]. Accurate measurements of the metabolic flux rate, using tracer infusion approaches, confirmed increased glycolysis along with suppressed tricarboxylic acid (TCA) cycle and oxidative phosphorylation (OXPHOS) in tumors compared to normal tissues [3]. Nevertheless, it has been known that glycolysis inhibitors do not exhibit the expected effects on suppressing tumor growth [4]. There is growing evidence that certain cancers show dependency on OXPHOS to produce energy for survival [5–7]. Bartman's analysis also showed that tumors generate most ATP through the TCA cycle/OXPHOS, even if their glycolytic activity is higher than that of normal tissues [3]. Recent findings have demonstrated that OXPHOS

Abbreviations: CI, respiratory complex I; OXPHOS, oxidative phosphorylation; I-BP-EG, 4′-iodobiphenyl ethylene glycol; EG, ethylene glycol; HIOP, 4-hydroxy-4′-iodobiphenyl.

* Corresponding author. Department of Materials and Applied Chemistry, College of Science and Technology, Nihon University, Kanda-Surugadai, Chiyoda-ku, Tokyo, 101-8308, Japan.
** Corresponding author. Department of Anatomy, Nihon University School of Dentistry, 1-8-13 Kanda-Surugadai, Chiyoda-ku, Tokyo, 101-8310, Japan.
E-mail addresses: otsuki.joe@nihon-u.ac.jp (J. Otsuki), fujiwara.kyoko@nihon-u.ac.jp (K. Fujiwara).

https://doi.org/10.1016/j.bbrep.2025.101981
Received 27 December 2024; Received in revised form 14 March 2025; Accepted 14 March 2025

is enhanced during tumor progression and in chemotherapy-resistant tumors [8]. Increased OXPHOS dependence has also been reported as a hallmark of cancer stem cells [9,10]. These observations suggest that OXPHOS is a promising target for the treatment of cancer.

Recently, extensive studies have been conducted to develop OXPHOS inhibitors as potential therapeutics for cancer treatment. Among these, inhibitors targeting respiratory complex I (CI), which is enzyme constituting the electron transport chain, exhibit promising properties as anti-cancer agents [11]. Epidemiological studies have revealed that patients with diabetes taking the treatment agent metformin, which has been proven to inhibit CI, showed a lower incidence of tumors [12]. The anti-tumor activity of metformin and its derivatives, phenformin and IM156, has been confirmed in many types of tumors [13–15]. CI inhibitor BAY-87-2243, initially developed as an inhibitory agent for hypoxia inducible factor 1α at first, and its derivate IACS-010759 have been shown to inhibit tumor growth efficiently both in clinical and experimental studies [16,17]. The therapeutic potential of other CI inhibitors, such as ME344, FRV-1, and DX3-213B, has also been extensively studied [18–20]. Nonetheless, only a few OXPHOS inhibitors are suitable for clinical use. IACS-010759 was shown to cause peripheral neuropathy in patients with acute myeloid leukemia and advanced solid tumors in a phase I clinical trial [21]. Despite promising results in epidemiological studies, metformin has shown limited effects in clinical trials of different tumor types [22]. Therefore, there is a strong demand to develop low-toxicity OXPHOS inhibitors with effective anti-tumor properties.

4′-Iodobiphenyl nonaethylene glycol ether (9bw) is a newly reported small molecule, composed of a biphenyl unit and 9 ethylene glycol (EG) units. It has been observed that 9bw represses the growth of many types of cancer cells but not normal fibroblasts [23,24] (Fujiwara's unpublished data). Recently, we have found that 9bw lead apoptosis in cancer cells by suppressing the CI activity, ensuing a decreased ATP production [24]. We also found that 9bw inhibited tumor growth *in vivo* without adversely affecting animal health [24]. These observations suggested strongly that 9bw is a possible antitumor agent with few adverse effects. However, the exact molecular mechanisms by which 9bw acts on CI remain elusive, partially because there is little similarity in its chemical structure to that of other known CI inhibitors. To clarify the molecular structure critical for 9bw's function, we analyzed the effect of 9bw analogues 4′-iodobiphenyl ethylene glycol (I-BP-EG), which are I-BP-EG3, I-BP-EG6 and I-BP-EG12 containing 3, 6, and 12 EG units, respectively (Fig. 1A), and 4-hydroxy-4′-iodobiphenyl (HIOP), which is composed of a biphenyl unit with a OH group instead of the EG unit (Fig. 1B), on human oral squamous cell carcinoma (OSCC)-derived cell lines HSC4 and Ca9-22. The results showed that six EG units were sufficient to suppress CI activity by as much as 9bw, though they were not sufficient to suppress ATP production and cell growth to 9bw's extent.

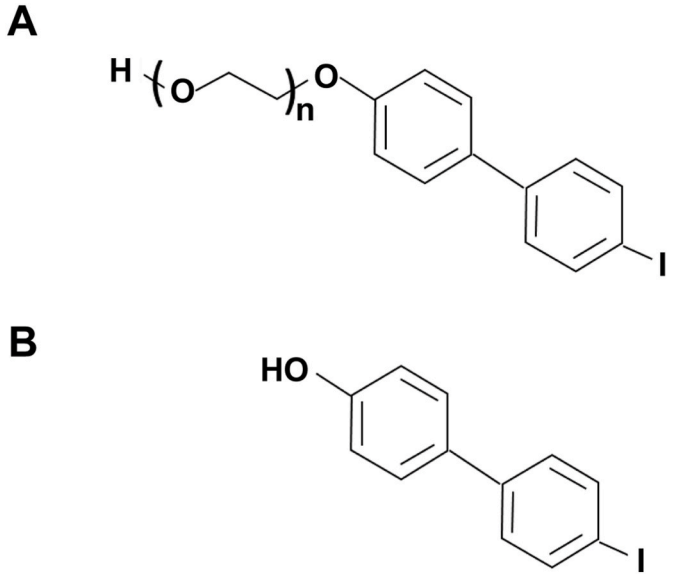

Fig. 1. Chemical structures of 9bw and its analogues. (A) The structures of 9bw and I-BP-EG. The value of n are 3, 6, 9 and 12 in I-BP-EG3, I-BP-EG6, 9bw and I-BP-EG12, respectively. (B) Stracture of HIOP.

2. Materials and methods

2.1. The compounds analyzed in this study

HIOP was purchased from Fujifilm Wako Pure Chemical Corporation (Osaka, Japan). I-BP-EG3 and I-BP-EG6 were synthesized using the methods described in Section 2.2. 9bw and I-BP-EG12 were kindly supplied by Mr. Naohisa Watanabe (Senka Pharmacy Co., Ltd). 9bw and I-BP-EG12 were hydrophilic, while HIOP, I-BP-EG3, and I-BP-EG6 were hydrophobic and insoluble in water. All compounds were dissolved in dimethyl sulfoxide to obtain 10 mM stock solutions, which were stored at −30 °C.

2.2. Synthesis of I-BP-EG3 and I-BP-EG6

The synthetic routes for I-BP-EG3 and I-BP-EG6 are depicted in Scheme 1 of the supplementary material (Figs. S1). Flash column chromatography was performed with Kanto Chemical silica gel (SiO_2) 60 N. NMR spectra were recorded with a JEOL JNM-ECX400 NMR spectrometer (400 MHz for ^{1}H and 100 MHz for ^{13}C). Electrospray mass spectrometry was performed by the Chemical Analysis Center of School of Pharmacy, Nihon University.

For the I-BP-EG3 synthesis, a solution of HIOP (502 mg, 1.69 mmol), $Cl(CH_2CH_2O)_3H$ (358 mg, 2.12 mmol), 20 % sodium ethoxide in ethanol (602 mg, 1.77 mmol), and potassium iodide (34 mg, 0.20 mmol) in ethanol (10 mL) was refluxed for 17 h. The solution was neutralized with 1 M HCl, concentrated, and dried under vacuum. The obtained solid was extracted with chloroform, which was washed with water, dried over magnesium sulfate, filtered, concentrated, and dried under vacuum. A part (50 mg) of the crude residue (749 mg) was chromatographed over silica gel eluted with ethyl acetate to afford a white solid (24 mg, 0.055 mmol, 49 %). ^{1}H NMR ($CDCl_3$): $\delta = 7.72$ (d, $J = 8.2$ Hz, 2H), 7.47 (d, $J = 8.7$ Hz, 2H), 7.28 (d, $J = 8.2$ Hz, 2H), 6.99 (d, $J = 8.7$ Hz, 2H), 4.17 (t, $J = 5.0$ Hz, 2H), 3.88 (t, $J = 5.0$ Hz, 2H), 2.39–3.76 (m, 6H), 3.62 (t, $J = 5.0$ Hz, 2H), 2.50 ppm (br, 1H); ^{13}C NMR ($CDCl_3$): δ = 158.6, 140.3, 137.8, 132.8, 128.6, 128.0, 115.1, 92.2, 72.6, 70.9, 70.4, 69.8, 67.5, 61.8 ppm; HRMS (ESI): *m/z* calcd for $C_{18}H_{22}O_4I + Na^+$: 451.0382 $[M+Na]^+$; found: 451.0385.

For the I-BP-EG6 synthesis, a mixture of HIOP (600 mg, 2.02 mmol) and 60 % sodium hydride (63 mg, 1.6 mmol) in tetrahydrofuran (2 mL) was stirred at room temperature under nitrogen for 1 h. To this mixture was added a solution of $Ts(OCH_2CH_2)_6OH$ (224 mg, 0.514 mmol) in tetrahydrofuran (3 mL) and the mixture was further stirred for 24 h. The mixture was diluted with ethyl acetate, washed with water and brine, dried over sodium sulfate, filtered, concentrated, and dried under vacuum. The residue was chromatographed over silica gel eluted with ethyl acetate and methanol (10:0 → 9:1) to afford a colorless oil (84 mg, 0.15 mmol, 7 %). ^{1}H NMR ($CDCl_3$): $\delta = 7.73$ (d, $J = 8.2$ Hz, 2H), 7.47 (d, $J = 8.7$ Hz, 2H), 7.29 (d, $J = 8.2$ Hz, 2H), 6.98 (d, $J = 8.7$ Hz, 2H), 4.17 (t, $J = 4.8$ Hz, 2H), 3.88 (t, $J = 4.8$ Hz, 2H), 3.63–3.76 (m, 18H), 3.60 ppm (t, $J = 2.9$ Hz, 2H); ^{13}C NMR ($CDCl_3$): δ = 158.8, 140.4, 137.8, 132.7, 128.7, 128.0, 115.1, 92.2, 72.7, 70.9, 70.7, 70.61, 70.57, 70.3, 69.8, 67.6, 61.8 ppm; HRMS (ESI): *m/z* calcd for $C_{24}H_{33}O_7I + Na^+$: 583.1169 $[M+Na]^+$; found: 583.1171.

2.3. Cell lines and culture conditions

The cell line HSC-4, which is derived from human tongue squamous

cell carcinoma, was purchased from the RIKEN Cell Bank (Ibaraki, Japan) The cell line Ca9-22, which is derived from human gingival squamous cell carcinoma, was purchased from the Health Science Research Resources Bank (Osaka, Japan). HSC-4 cells were cultured in RPMI-1640 medium (Nacalai Tesque, Kyoto, Japan) and Ca9-22 cells were cultured in minimal essential medium (MEM; Nacalai Tesque) supplemented with 600 mg/L glutamine. Both media contained 10 % heat-inactivated fetal bovine serum (FBS; Nichirei Bioscience, Tokyo, Japan), 100 IU/mL penicillin (Thermo Fisher Scientific, Waltham, MA, USA), and 100 mg/mL streptomycin (Thermo Fisher Scientific). The cells were maintained at 37 °C in humidified air containing 5 % CO_2.

2.4. Analysis of cell viability

To analyze the effects of the compounds on cell viability, a water-soluble tetrazolium salt (WST)-8 assay was performed by following manufacture's instruction. Briefly, cells were plated in 96-well culture plates at a density of 1×10^3 cells/well and the medium was replaced with a fresh medium containing various concentrations of the compounds after 24 h. The cells were cultured for 72 h and the medium was replaced with 10 % (V/V) solution of Cell Count Reagent CF (Nacalai Tesque) diluted in fresh medium. After culturing cells for additional 1 h, the absorbance at OD450 nm was measured by plate reader.

2.5. Measurement of intracellular ATP amount

Intracellular ATP level was measured using an ATP assay kit (TOYO-B-Net, Tokyo, Japan), according to the manufacturer's instructions. In Brief, the cells were plated in 96-well plates at a density of 5×10^3 cells/well, cultured for 24 h, and the culture medium was replaced with a fresh medium with or without 1 μM of each compound. After 12-h incubation, cell extracts were mixed with the solution containing luciferase and luminescence intensity of the mixtures were monitored using a luminometer to measure intracellular ATP level.

2.6. Measurement of the activity of CI in isolated mitochondria

Mitochondria were isolated using Mitochondria Isolation Kit (ab288084; Abcam), by following the manufacturer's instructions with some modification. Briefly, HSC4 and Ca9-22 cells grown to approximately 90 % confluency in dishes 100 mm in diameter were washed twice with PBS, scraped, and collected with PBS. Cells were precipitated by centrifugation at 200×*g* at room temperature, and the pellets of the cells were suspended in mitochondrial isolation buffer, followed by homogenization on ice for five strokes using a Dounce homogenizer. The homogenates were passed through a 27G needle attached to 1-mL syringe for 5 times and centrifuged at 700×*g* at 4 °C for 10 min to remove debris. The supernatants were collected and centrifuged at 6000×*g* at 4 °C for 10 min. The precipitated mitochondria were washed again with the buffer solution and then suspended in nine volumes of storage buffer provided in the kit.

The effects of the compounds on CI activity were determined as previously described [25] with some modifications. Briefly, mitochondria with 5-μg protein were suspended in Mitochondrial Complex I Activity Assay Buffer (700931; Cayman Chemical, Ann Arbor, MI), supplemented with 2 mM KCN, 2.5 mg/mL bovine serum albumin, 130 μM albumin, 65 μM decyl ubiquinone, 2 μg/mL antimycin A and 1 μM of each compound or medium. After mixing all the reactants in 96 well half-area plate, the absorbance of NADH at 340 nm was measured every minute for 15 min. The absorbance at 425 nm was also measured simultaneously at the same time as a reference. The reduction rate of the values obtained by subtracting the reference wavelength from absorbance at 340 nm was calculated to determine CI activity.

2.7. Detection of the compound incorporated into mitochondria by HPLC

To detect the incorporation of 9bw and its analogues into the mitochondria, HSC4 cells were plated at a density of 5×10^5 cells/dish in culture dishes 100 mm in diameter. Three dishes were prepared for each experiment. Twenty-four hours after the seeding, 10 μM of each compound was added to the dishes, and the cells were cultured for an additional 2 h. Then mitochondria were isolated by the method described in section 2.6 with some modification. Briefly, after washing once with PBS, the cells were scraped and collected with PBS. Subsequently, the cells were precipitated by centrifugation at 200×*g* at room temperature, and the cell pellet was suspended in 1 mL of mitochondria isolation buffer, followed by homogenization by passing through a 1-mL syringe with a 27G needle 10 times. The homogenates were centrifuged at 700×*g* at 4 °C for 10 min and the supernatants were centrifuged in new tubes at 6000×*g* at 4 °C for 10 min. The precipitated mitochondria were treated with 50 μl of 0.1 % trifluoroacetic acid (TFA) in acetonitrile (ACN) and the extracts were collected by centrifugation at 6000×*g*. The supernatant was mixed with 150 μl 0.1 % TFA in distilled water, followed by the filtration through 0.2 μm IC Millex Filter Unit (MilliporeSigma, Burlington, MA).

The filtered extracts were analyzed by reverse phase high-performance liquid chromatography (HPLC), by following the previous report with some modifications [26]. Briefly, the analysis was performed using an HPLC system consisting of 305/306 pumps, a 502 degasser, an 811D mixer, an 805 manometric module, and a155 UV/Vis detector (Gilson, Middleton, WI). All measurements and data analyses were performed using UniProt Software version 5.11 (Gilson). Columns used in this analysis was Jupiter 15 μm C18 column 300 Å 250 × 4.6 mm (Phenomenex, Torrance, CA) attached to a μBondapak C18 Guard-Pak Insert guard column (Waters, Milford, MA). The solvent system was a 1:1 mixture of 0.1 % TFA in water and 0.1 %TFA in ACN at a flow rate of 1.0 mL/min. Absorbance at 270 nm was monitored to detect 9bw and its analogues.

2.8. Statistical analysis

One-way ANOVA, followed by post-hoc Dunnett's test was executed to examine the significance of the differences between the control and treatment groups. JMP software ver. 11.2 (SAS Institute Inc., Cary, NC) was used for statistical analysis. Data was presented as the means ± SD of independent experiments performed for three times or more. In all analyses, $P < 0.05$ was considered as statistically significant. The IC_{50} values for each compound were obtained based on a nonlinear regression curve, calculated using JMP.

3. Results

3.1. Number of EG units affected viability of cells

To examine the effect of the number of EG units in 9bw and its analogues on cell viability, human OSCC-derived HSC-4 and Ca9-22 cells were cultured in the presence or absence of various concentrations of 9bw and its analogues. Although WST-8 cell survival assay showed that all I-BP-EGs suppressed cell viability, 9bw and I-BP-EG12 showed stronger effects than I-BP-EG3 and I-BP-EG6 (Fig. 2). IC_{50} values for I-BP-EG3, I-BP-EG6, 9bw and I-BP-EG12 were 1.27 μM, 0.53 μM, 0.0065 μM, and 0.021 μM, respectively in HSC-4 cells (Fig. 2A). That were 1.28 μM, 2.27 μM, 0.125 μM and 0.564 μM, respectively in Ca9-22 cells (Fig. 2B). HIOP hardly affected cell viability in HSC4 and had only a minimal effect on Ca9-22 at 10 μM or lower concentrations. IC_{50} values for HIOP were higher than 50 μM in both cells.

3.2. HIOP and I-BP-EG3 did not reduce intracellular ATP

As 9bw reduces the amount of intracellular ATP by inhibiting the CI

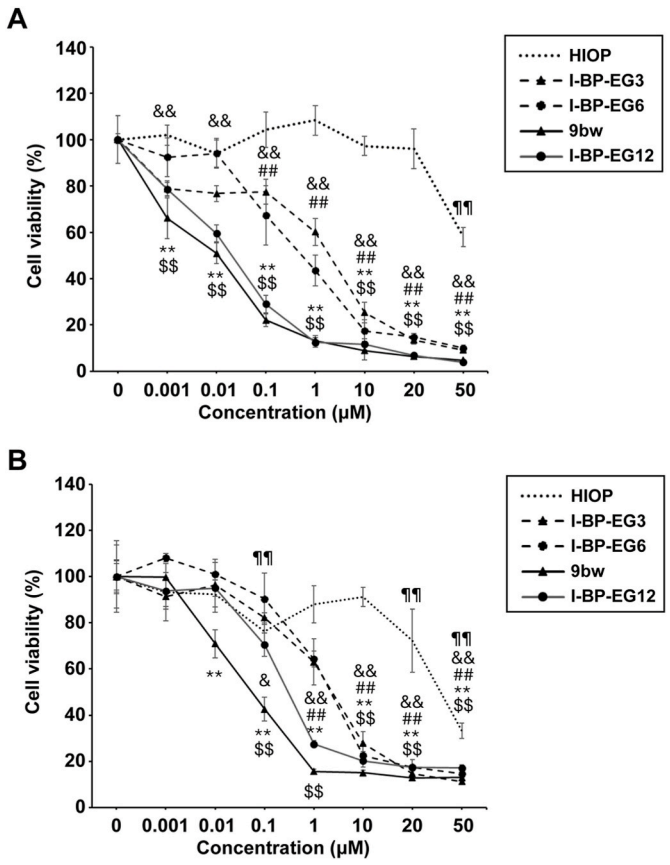

Fig. 2. Effects of treatment with 9bw or its analogues on the viability of OSCC-derived HSC-4 and Ca9-22 cells. HSC-4 (A) and Ca9-22 (B) cells were treated with 9bw or its analogues at the indicated concentrations. Three days after treatment, the cell viability was measured using the WST-8 assay. Data are presented as the means ± SD of quadruplicate measurements. & $P < 0.05$ for I-BP-EG3; ¶¶, &&, ##, **, $$ $P < 0.01$ for HIOP, I-BP-EG3, I-BP-EG6, 9bw and I-BP-EG12, respectively.

activity [24], the effects of 9bw's analogues on intracellular ATP were also analyzed. It was demonstrated that 1 μM of 9bw and I-BP-EG12 significantly reduced the amount of ATP both in HSC-4 (Fig. 3A) and Ca9-22 cells (Fig. 3B), though I-BP-EG3 and HIOP did not show any effect on ATP (Fig. 3). I-BP-EG6 reduced the ATP levels to approximately 80 % of the control levels; however, this difference was not statistically significant.

3.3. I-BP-EG6 and I-BP-EG12 inhibited CI to the same extent as 9bw did

Next, the effects of 9bw and its analogues on the CI activity were examined. Mitochondria were isolated from HSC-4 and Ca9-22 cells, and the CI activity in these mitochondria was measured in the presence or absence of 1 μM of the compounds. As shown in Fig. 4, both HSC-4 and Ca9-22 derived mitochondria incubated with 1 μM of I-BP-EG6, 9bw and I-BP-EG12 showed significantly lower CI activity than those in the control condition. The enzymatic activities with I-BP-EG6, 9bw and I-BP-EG12 were approximately 50 % compared to the control in HSC-4 derived mitochondria (Figs. 4A) and 60 % in Ca9-22 derived (Fig. 4B). In contrast, HIOP and I-BP-EG3 had little effect on CI activity in HSC-4 mitochondria (Fig. 4A). The activity was approximately 80 % of that of the control in Ca9-22 derived mitochondria with HIOP or I-BP-EG3, but the reduction was not statistically significant (Fig. 4B).

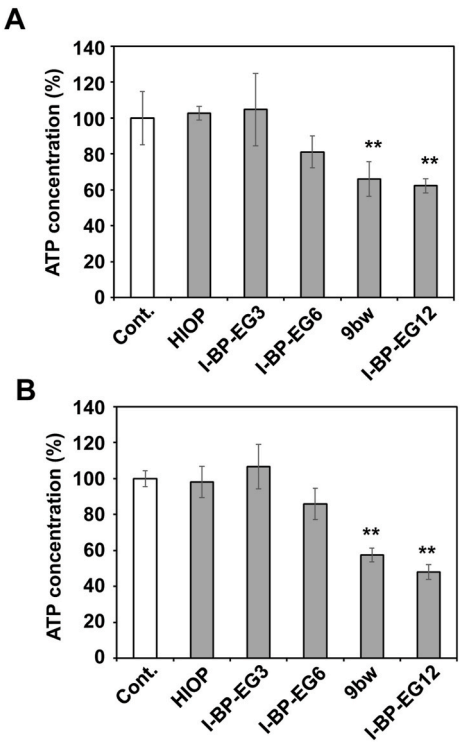

Fig. 3. Effects of treatment with 9bw or its analogues on intracellular ATP concentration. HSC-4 (A) and Ca9-22 (B) cells were treated witn 1 μM of 9bw or its analogues for 12 h followed by the measurement of intracellular ATP concentraton. Data are presented as the means ± SD of quadruplicate measurements. $**P < 0.01$.

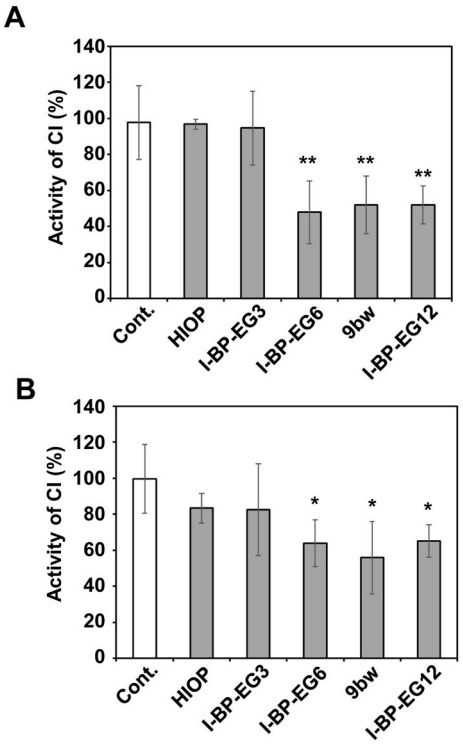

Fig. 4. Effects of the treatment with 9bw or its analogues on the activity of CI. Mitochondria was isolated from HSC-4 (A) and Ca9-22 (B) cells and the activity of CI in those mitochondria was measured in the presence or absense of 1 μM of 9bw or its analogues. Data are presented as the means ± SD of quadruplicate measurements. $*P < 0.05$, $**P < 0.01$.

3.4. All compounds except for I-BP-EG12 were shown to be incorporated into mitochondria

There are two possible explanations for the inability of I-BP-EG3 and HIOP to inhibit CI activity: either these compounds cannot be incorporated into the mitochondria, or, even if they are incorporated, they are unable to affect CI. To distinguish between these possibilities, we examined the accumulation of these compounds in the mitochondria of HSC4 cells by HPLC. As there were many mitochondria-derived molecules whose retention times were similar to those of 9bw and its analogues in Ca9-22 cells, the analyses were performed only for HSC4 cells. After incubation of the cells in the presence or absence of 10 μM compounds for 2 h, mitochondria were isolated from the cells, and extracts from the mitochondria were subjected to analysis. As standard 0.1 μM 9bw and its analogues could be detected by monitoring absorbance at 270 nm (Fig. 5A), mitochondrial extracts were analyzed in the same condition. The chromatogram clearly indicated that all the compounds except I-BP-EG12 were incorporated into the mitochondria (Fig. 5B). I-BP-EG12 was not detected in the mitochondrial extracts because there were peaks derived from mitochondrial intrinsic molecules at approximately 12–13 min, which is close to the retention time of I-BP-EG12. Among the compounds other than I-BP-EG12, a larger number of EG units demonstrated a smaller peak area.

4. Discussion

The present data clearly demonstrate that the number of EG units in 9bw and its analogues is critical for their inhibitory effects on CI. Compounds with six or more EG units inhibited CI almost equally. However, HIOP and I-BP-EG3 did not show any inhibitory effects on CI. As HPLC analyses indicated that both HIOP and I-BP-EG3 could be abundantly incorporated into the mitochondria, the lack of their inhibitory effects on CI was not due to their absence within the mitochondria. In contrast, the HPLC analysis demonstrated that a longer EG

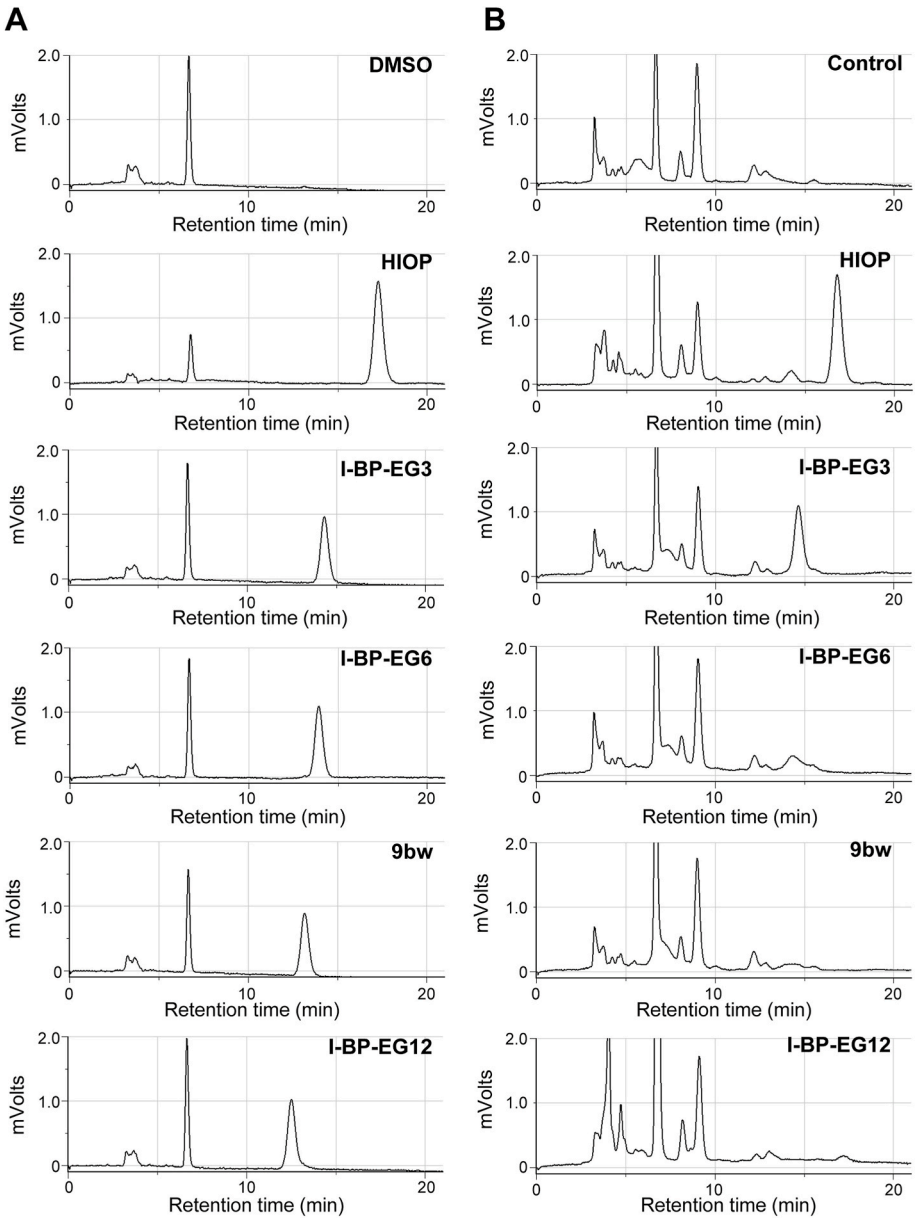

Fig. 5. Uptake of 9bw or its analogues by mitochondria. HSC-4 cells were incubated with 10 μM of 9bw or its analogues for 2 h, followed by the isolation of mitochondria from them. Extracts from the mitochondria were subjected to HPLC analysis to determine the content of the compounds. Chromatograms for 0.1 μM standard solution of each compound (A) and representative chromatograms for mitochondrial extracts (B) are shown.

chain was associated with lower amounts of the compounds in the mitochondria. Although 9bw and I-BP-EG12 significantly inhibited CI, the analysis detected very low amounts of 9bw in the mitochondria. The I-BP-EG12 specific peak was hardly detected among the peaks of the mitochondria-derived molecules. This may be attributed to water solubility of them. As mentioned above, 9bw and I-BP-EG12 are hydrophilic, whereas I-BP-EG3, I-BP-EG6 and HIOP are hydrophobic. During the mitochondrial isolation, cells are suspended in buffers in several steps. We speculate that 9bw and I-BP-EG12 were washed out of the mitochondria during the process. To directly quantify the amount of the compound in the mitochondria, we are now developing fluorescently labeled 9bw and its analogues to observe the compounds incorporated into the mitochondria via microscopy.

The mechanisms underlying the inhibition of CI by 9bw have not been elucidated. The chemical structure of 9bw has little similarity to those of other CI inhibitors such as rotenone, metformin, and ME344. CI has an L-shaped structure consisting of a hydrophilic domain facing into the mitochondrial matrix and a hydrophobic domain located within the inner mitochondrial membrane [27]. Electron transfer occurs in the hydrophilic domain, while proton translocation occurs in the hydrophobic domain [27]. CI catalyzes the transport of two electrons from NADH to ubiquinone and resulting four protons are translocated to the mitochondrial intermembrane space, generating a concentration gradient of proton across the inner membrane. Electrons from NADH are transferred to flavin mononucleotide (FMN) and transferred to ubiquinone within the Q-tunnel through a sequence of iron-sulfur clusters [28]. Although there are a few inhibitors bind to the FMN sites, most CI inhibitors exert their effects by blocking the quinone-binding site in the Q-tunnel [29]. A recent study using cryo-electron microscopy revealed that rotenone has two binding sites in Q-tunnel [30]. Analysis of the mutations found in IACS-10759 resistant cells clarified that IACS-10759 binds to the ND1 subunit, which is located at the entrance of the Q-tunnel [16]. Because 9bw has a long EG chain, it is speculated that 9bw may enter the Q-tunnel as decyl ubiquinone, which has saturated decyl hydrocarbon chain, or as ubiquinone with a long isoprenoid side chain. Because I-BP-EG3 had no inhibitory effect on CI, we speculated that the three EGs may not be sufficiently long to occupy the Q-tunnel. Molecular docking analysis at the quinone-binding site, has been identified and analyzed through computer simulations [31,32], suggested that the 4′-iodo-biphenyl moiety of 9bw and its analogues located at the entry portal of the Q-tunnel formed by transmembrane helices (TMHs) 1 and 6 and surface helix α1 of subunit ND1 (hydrophobic sites 4 and 5, Figs. S2 and S3, Table S1) [33]. All compounds adopted the same docking mode, indicating that the results were highly reliable. These results suggest that HIOP and I-BP-EG3 may not be sufficiently long to reach the Q redox-active site near N2. Further investigations are needed to clarify the exact binding site of 9bw on CI using cryo-electron microscopy or photoaffinity labeling technique [34].

In the current study, I-BP-EG6 significantly suppressed cell viability and reduced the intracellular amount of ATP to some extent, but not as much as 9bw or I-BP-EG12, although all these three compounds inhibited CI almost equally. Since cell viability and ATP assays were conducted on whole cells, whereas CI inhibition was assessed using isolated mitochondria, we initially hypothesized that I-BP-EG6 might not be sufficiently incorporated into cells. However, the HPLC analysis did not confirm this possibility. Another possibility is that 9bw and I-BP-EG12 have additional targets other than CI. A previous observation that 9bw strongly reduced the intracellular amount of ATP in cancer cells, but not in normal cells, although 9bw suppressed the oxygen consumption rate of both cancer and normal cells equally, supports this hypothesis [24]. Additionally, I-BP-EG3 suppressed cell growth to the same extent as I-BP-EG6, although I-BP-EG3 did not reduce the CI activity nor intracellular ATP levels. These observations indicated that I-BP-EG3 affects cell viability by inhibiting or activating unknown target (s) other than OXPHOS or glycolysis. The mechanism by which I-BP-EG3 suppresses cell growth and other characteristics of this compound, such as its toxicity to normal cells and living animals, will be tested to evaluate whether I-BP-EG3 can be developed as an antitumor agent.

Although CI has been studied extensively for several decades, the precise molecular mechanisms of its catalytic action have not been completely elucidated. This is mainly due to the complex structure of CI, which has a molecular weight 1 MDa, comprising 45 subunits in mammals [35]. Recent studies using cryo-electron microscopy and photoaffinity probes have been elucidating the detailed catalytic mechanisms of CI gradually [29]. For these studies, CI inhibitors were used to reveal the exact structure and conformational changes of the catalytic site in CI. We believe that further studies to identify the binding site of 9bw and its analogues on CI will also help us understand the exact catalytic mechanisms of CI.

Taken together, our results showed that the number of EG units is critical for the inhibitory effect of 9bw analogues on CI. It was demonstrated that six EG units were sufficient for I-BP-EGs to suppress the CI activity by as much as 9bw, though three EG units did not have an inhibitory effect.

CRediT authorship contribution statement

Kazuaki Sekimoto: Visualization, Investigation, Formal analysis. **Hanaka Kinjo:** Resources, Investigation. **Mizuki Murakami:** Resources, Investigation. **Akiko Ohashi:** Resources, Investigation. **Rei Fukui:** Investigation, Formal analysis. **Eri Nagasaki-Maeoka:** Writing – review & editing, Investigation. **Yoshinori Inagaki:** Investigation, Formal analysis. **Tadateru Takayama:** Writing – review & editing, Project administration. **Kazuhiro Ikeda:** Writing – review & editing, Data curation. **Ken-ichi Takayama:** Writing – review & editing, Data curation. **Satoshi Inoue:** Writing – review & editing, Supervision. **Motonori Tsuji:** Writing – review & editing, Visualization, Validation, Investigation, Formal analysis. **Joe Otsuki:** Writing – review & editing, Visualization, Validation, Supervision, Resources, Project administration, Investigation. **Kyoko Fujiwara:** Writing – original draft, Visualization, Supervision, Project administration, Investigation, Funding acquisition, Formal analysis, Data curation, Conceptualization.

Funding

This study was supported in part by KAKENHI (grant number 22K09931) to Kyoko Fujiwara, grant from the Dental Research Center, Nihon University School of Dentistry (2022), and Uemura Fund, Nihon University School of Dentistry (UEMURA-2023-1, UEMURA-2024-1) to Kyoko Fujiwara.

Declaration of competing interest

The authors declare that they have no known competing financial interests or personal relationships that could have appeared to influence the work reported in this paper.

Acknowledgments

We are grateful to Dr. Masakazu Sekijima and Dr. Kazuki Yamamoto for their useful suggestions and discussion. We are grateful to Mr. Yusaku Kobayashi for his help with the synthesis of the compounds used in this study. We also thank Editage (www.editage.jp) for helping us English language editing.

Appendix A. Supplementary data

Supplementary data to this article can be found online at https://doi.org/10.1016/j.bbrep.2025.101981.

Data availability

The data that has been used is confidential.

References

[1] O. Warburg, Injuring of respiration the origin of cancer cells, Science 123 (1956) 309–314, https://doi.org/10.1126/science.123.3191.309.

[2] J. Schiller, V. Zickermann, Binding of natural inhibitors to respiratory complex I, Pharmaceuticals 15 (2022) 1088, https://doi.org/10.3390/ph15091088.

[3] C.R. Bartman, D.R. Weilandt, Y. Shen, W.D. Lee, Y. Han, T. TeSlaa, C.S. R. Jankowski, L. Samarah, N.R. Park, V. da Silva-Diz, M. Aleksandrova, Y. Gultekin, A. Marishta, L. Wang, L. Yang, A. Roichman, V. Bhatt, T. Lan, Z. Hu, X. Xing, W. Lu, S. Davidson, M. Wühr, M.G. Vander Heiden, D. Herranz, J.Y. Guo, Y. Kang, J.D. Rabinowitz, Slow TCA flux and ATP production in primary solid tumours but not metastases, Nature 614 (2023) 349–357, https://doi.org/10.1038/s41586-022-05661-6.

[4] D. DeWaal, V. Nogueira, A.R. Terry, K.C. Patra, S.M. Jeon, G. Guzman, J. Au, C. P. Long, M.R. Antoniewicz, N. Hay, Hexokinase-2 depletion inhibits glycolysis and induces oxidative phosphorylation in hepatocellular carcinoma and sensitizes to metformin, Nat. Commun. 9 (2018) 446, https://doi.org/10.1038/s41467-017-02733-4.

[5] J. Hu, J.W. Locasale, J.H. Bielas, J. O'Sullivan, K. Sheahan, L.C. Cantley, M.G. V. Heiden, D. Vitkup, Heterogeneity of tumor-induced gene expression changes in the human metabolic network, Nat. Biotechnol. 31 (2013) 522–529, https://doi.org/10.1038/nbt.2530.

[6] A. Roesch, A. Vultur, I. Bogeski, H. Wang, K.M. Zimmermann, D. Speicher, C. Körbel, M.W. Laschke, P.A. Gimotty, S.E. Philipp, E. Krause, S. Pätzold, J. Villanueva, C. Krepler, M. Fukunaga-Kalabis, M. Hoth, B.C. Bastian, T. Vogt, M. Herlyn, Overcoming intrinsic multidrug resistance in melanoma by blocking the mitochondrial respiratory chain of slow-cycling JARID1Bhigh cells, Cancer Cell 23 (2013) 811–825, https://doi.org/10.1016/j.ccr.2013.05.003.

[7] S. Sriskanthadevan, D.V. Jeyaraju, T.E. Chung, S. Prabha, W. Xu, M. Skrtic, B. Jhas, R. Hurren, M. Gronda, X. Wang, Y. Jitkova, M.A. Sukhai, F.H. Lin, N. Maclean, R. Laister, C.A. Goard, P.J. Mullen, S. Xie, L.Z. Penn, I.M. Rogers, J.E. Dick, M. D. Minden, A.D. Schimmer, AML cells have low spare reserve capacity in their respiratory chain that renders them susceptible to oxidative metabolic stress, Blood 125 (2015) 2120–2130, https://doi.org/10.1182/blood-2014-08-594408.

[8] V. Sica, J.M. Bravo-San Pedro, G. Stoll, G. Kroemer, Oxidative phosphorylation as a potential therapeutic target for cancer therapy, Int. J. Cancer 146 (2020) 10–17, https://doi.org/10.1002/ijc.32616.

[9] P. Sancho, D. Barneda, C. Heeschen, Hallmarks of cancer stem cell metabolism, Br. J. Cancer 114 (2016) 1305–1312, https://doi.org/10.1038/bjc.2016.152.

[10] E.M. Kuntz, P. Baquero, A.M. Michie, K. Dunn, S. Tardito, T.L. Holyoake, G. V. Helgason, E. Gottlieb, Targeting mitochondrial oxidative phosphorylation eradicates therapy-resistant chronic myeloid leukemia stem cells, Nat. Med. 23 (2017) 1234–1240, https://doi.org/10.1038/nm.4399.

[11] T.M. Ashton, W. Gillies McKenna, L.A. Kunz-Schughart, G.S. Higgins, Oxidative phosphorylation as an emerging target in cancer therapy, Clin. Cancer Res. 24 (2018) 2482–2490, https://doi.org/10.1158/1078-0432.CCR-17-3070.

[12] R.A. Miller, Q. Chu, J. Xie, M. Foretz, B. Viollet, M.J. Birnbaum, Biguanides suppress hepatic glucagon signalling by decreasing production of cyclic AMP, Nature 494 (2013) 256–260, https://doi.org/10.1038/nature11808.

[13] S.Y. Rha, S.-H. Beom, Y.G. Shin, D.-S. Yim, Y.W. Moon, T.W. Kim, S.Y. Kim, G. M. Kim, H.S. Kim, J.-H. Cheong, Y.W. Lee, B.J. Geiger, S. Yoo, M.S. Rudoltz, F. Janku, Phase I study of IM156, a novel potent biguanide oxidative phosphorylation (OXPHOS) inhibitor, in patients with advanced solid tumors, J. Clin. Oncol. 38 (2020) 3590, https://doi.org/10.1200/jco.2020.38.15_suppl.3590.

[14] W.W. Wheaton, S.E. Weinberg, R.B. Hamanaka, S. Soberanes, L.B. Sullivan, E. Anso, A. Glasauer, E. Dufour, G.M. Mutlu, G.R. Scott Budigner, N.S. Chandel, Metformin inhibits mitochondrial complex I of cancer cells to reduce tumorigenesis, Elife 2014 (2014) e02242, https://doi.org/10.7554/eLife.02242.

[15] H.R. Bridges, A.J.Y. Jones, M.N. Pollak, J. Hirst, Effects of metformin and other biguanides on oxidative phosphorylation in mitochondria, Biochem. J. 462 (2014) 475–487, https://doi.org/10.1042/BJ20140620.

[16] J.R. Molina, Y. Sun, M. Protopopova, S. Gera, M. Bandi, C. Bristow, T. McAfoos, P. Morlacchi, J. Ackroyd, A.N.A. Agip, G. Al-Atrash, J. Asara, J. Bardenhagen, C. C. Carrillo, C. Carroll, E. Chang, S. Ciurea, J.B. Cross, B. Czako, A. Deem, N. Daver, J.F. De Groot, J.W. Dong, N. Feng, G. Gao, J. Gay, M.G. Do, J. Greer, V. Giuliani, J. Han, L. Han, V.K. Henry, J. Hirst, S. Huang, Y. Jiang, Z. Kang, T. Khor, S. Konoplev, Y.H. Lin, G. Liu, A. Lodi, T. Lofton, H. Ma, M. Mahendra, P. Matre, R. Mullinax, M. Peoples, A. Petrocchi, J. Rodriguez-Canale, R. Serreli, T. Shi, M. Smith, Y. Tabe, J. Theroff, S. Tiziani, Q. Xu, Q. Zhang, F. Muller, R.A. Depinho, C. Toniatti, G.F. Draetta, T.P. Heffernan, M. Konopleva, P. Jones, M.E. Di Francesco, J.R. Marszalek, An inhibitor of oxidative phosphorylation exploits cancer vulnerability, Nat. Med. 24 (2018) 1036–1046, https://doi.org/10.1038/s41591-018-0052-4.

[17] A. Tsuji, T. Akao, T. Masuya, M. Murai, H. Miyoshi, IACS-010759, a potent inhibitor of glycolysis-deficient hypoxic tumor cells, inhibits mitochondrial respiratory complex I through a unique mechanism, J. Biol. Chem. 295 (2020) 7481–7491, https://doi.org/10.1074/jbc.RA120.013366.

[18] M. Quintela-Fandino, S. Morales, A. Cortes-Salgado, L. Manso, J.V. Apala, M. Muñoz, A.G. Cudos, J.S. Fortuny, M. Gion, A. Lopez-Alonso, J. Cortes, J. Guerra, D. Malon, E. Caleiras, F. Mulero, S. Mouron, Randomized phase 0/I trial of the mitochondrial inhibitor Me-344 or placebo added to bevacizumab in early HER2-negative breast cancer, Clin. Cancer Res. 26 (2020) 35–45, https://doi.org/10.1158/1078-0432.CCR-19-2023.

[19] M. Monroy-Cárdenas, V. Andrades, C. Almarza, M.J. Vera, J. Martínez, R. Pulgar, J. Amalraj, R. Araya-Maturana, F.A. Urra, A new quinone-based inhibitor of mitochondrial complex I in D-conformation, producing invasion reduction and sensitization to venetoclax in breast cancer cells, Antioxidants 12 (2023) 1597, https://doi.org/10.3390/antiox12081597.

[20] T. Sun, Z. Yan, J. Cai, X. Shao, D. Wang, Y. Ding, Y. Feng, J. Yang, E. Luo, X. Feng, D. Jing, Effects of mechanical vibration on cell morphology, proliferation, apoptosis, and cytokine expression/secretion in osteocyte-like MLO-Y4 cells exposed to high glucose, Cell Biol. Int. 44 (2019) 216–228, https://doi.org/10.1002/cbin.11221.

[21] T.A. Yap, N. Daver, M. Mahendra, J. Zhang, C. Kamiya-Matsuoka, F. Meric-Bernstam, H.M. Kantarjian, F. Ravandi, M.E. Collins, M.E. Di Francesco, E. E. Dumbrava, S. Fu, S. Gao, J.P. Gay, S. Gera, J. Han, D.S. Hong, E.J. Jabbour, Z. Ju, D.D. Karp, A. Lodi, J.R. Molina, N. Baran, A. Naing, M. Ohanian, S. Pant, N. Pemmaraju, P. Bose, S.A. Piha-Paul, J. Rodon, C. Salguero, K. Sasaki, A.K. Singh, V. Subbiah, A.M. Tsimberidou, Q.A. Xu, M. Yilmaz, Q. Zhang, Y. Li, C.A. Bristow, M.B. Bhattacharjee, S. Tiziani, T.P. Heffernan, C.P. Vellano, P. Jones, C.J. Heijnen, A. Kavelaars, J.R. Marszalek, M. Konopleva, Complex I inhibitor of oxidative phosphorylation in advanced solid tumors and acute myeloid leukemia: phase I trials, Nat. Med. 29 (2023) 115–126, https://doi.org/10.1038/s41591-022-02103-8.

[22] S.R. Lord, A.L. Harris, Is it still worth pursuing the repurposing of metformin as a cancer therapeutic? Br. J. Cancer 128 (2023) 958–966, https://doi.org/10.1038/s41416-023-02204-2.

[23] Senka Pharmacy Co, Ltd. Polyethylene Glycol Derivatives and Anticancer Drugs Containing Them, JP5364532B2, 2013, 12–11.

[24] E. Nagasaki-Maeoka, K. Ikeda, K. ichi Takayama, T. Hirano, Y. Ishizuka, T. Koshinaga, N. Tsukune, T. Takayama, S. Inoue, K. Fujiwara, Polyethylene glycol derivative 9bw suppresses growth of neuroblastoma cells by inhibiting oxidative phosphorylation, Cancer Sci. 111 (2020) 2943–2953, https://doi.org/10.1111/CAS.14512.

[25] M.A. Birch-Machin, D.M. Turnbull, Assaying mitochondrial respiratory complex activity in mitochondria isolated from human cells and tissues, Methods Cell Biol. 65 (2001) 97–117, https://doi.org/10.1016/s0091-679x(01)65006-4.

[26] S. Uno, A.H. Harkiss, R. Chowdhury, S.T. Caldwell, T.A. Prime, A.M. James, B. Gallagher, J. Prudent, R.C. Hartley, M.P. Murphy, Incorporating a polyethyleneglycol linker to enhance the hydrophilicity of mitochondria-targeted triphenylphosphonium constructs, Chembiochem 24 (2023) e202200774, https://doi.org/10.1002/cbic.202200774.

[27] C. Wirth, U. Brandt, C. Hunte, V. Zickermann, Structure and function of mitochondrial complex i, Biochim. Biophys. Acta, Bioenerg. 1857 (2016) 902–914, https://doi.org/10.1016/j.bbabio.2016.02.013.

[28] J. Hirst, Mitochondrial complex I, Annu. Rev. Biochem. 82 (2013) 551–575, https://doi.org/10.1146/ANNUREV-BIOCHEM-070511-103700.

[29] M. Murai, Exploring the binding pocket of quinone/inhibitors in mitochondrial respiratory complex I by chemical biology approaches, Biosci. Biotechnol. Biochem. 84 (2020) 1322–1331, https://doi.org/10.1080/09168451.2020.1747974.

[30] D. Kampjut, L.A. Sazanov, The coupling mechanism of mammalian respiratory complex I, Science 370 (2020) 6516, https://doi.org/10.1126/SCIENCE.ABC4209.

[31] O. Haapanen, A. Djurabekova, V. Sharma, Role of second quinone binding site in proton pumping by respiratory complex I, Front. Chem. 7 (2019) 221, https://doi.org/10.3389/fchem.2019.00221.

[32] A. Djurabekova, E.G. Yoga, A. Nyman, A. Pirttikoski, V. Zickermann, O. Haapanen, V. Sharma, Docking and molecular simulations reveal a quinonebinding site on the surface of respiratory complex I, FEBS (Fed. Eur. Biochem. Soc.) Lett. 596 (2022) 1133–1146, https://doi.org/10.1002/1873-3468.14346.

[33] E.G. Yoga, J. Schiller, V. Zickermann, Ubiquinone binding and reduction by complex I—open questions and mechanistic implications, Front. Chem. 9 (2021) 672851, https://doi.org/10.3389/fchem.2021.672851.

[34] Y. Hatanaka, Y. Sadakane, Photoaffinity labeling in drug discovery and developments: chemical gateway for entering proteomic frontier, Curr. Top. Med. Chem. 2 (2005) 271–288, https://doi.org/10.2174/1568026023394182.

[35] L.A. Sazanov, From the "black box" to "domino effect" mechanism: what have we learned from the structures of respiratory complex i, Biochem. J. 480 (2023) 319–333, https://doi.org/10.1042/BCJ20210285.